STEADY STATE TEMPERATURE PROFILE IN A CYLINDER HEATED BY MICROWAVES

H.W. Jackson, M. Barmatz, and P. Wagner
Jet Propulsion Laboratory, California Institute of Technology
Pasadena, CA 91109

ABSTRACT

We have developed a new theory to calculate the steady state temperature profile in a cylindrical sample positioned along the entire axis of a cylindrical microwave cavity. Temperature profiles were computed for alumina rods of various radii contained in a cavity excited in one of the TM_{0n0} modes with n = 1, 2 or 3. Sample surface and center temperatures will be presented as a function of total sample absorbed power or electric field strength at the sample surface. An approach for attaining more uniform heating within the sample by reducing the magnitude of the inverted temperature profile using a concentric outer cylindrical tube will be discussed. Also, parametric studies will be reported for model calculations in which the total hemispherical emissivity was varied at boundaries of the sample and surrounding tube and at the cavity wall. The results will be discussed in the context of controlling both the average sample temperature and the temperature distribution in the sample during microwave processing.

INTRODUCTION

Realistic models of microwave cavity reactors that provide accurate and rapid predictions of thermal and electromagnetic characteristics for materials processing have been developed recently. Some features of the models will be described in this paper, and calculated results that demonstrate their usefulness will be presented. The results can be applied in exploring new configurations for microwave reactors, predicting and controlling processing conditions, and designing and optimizing new reactors.

In previous work [1,4]we have treated a spherical sample in a rectangular cavity using a spherical shell mode] for the sample. Electromagnetic fields were calculated using methods that were improvements over ordinary cavity perturbation theory, but which still were not exact. Results of the electromagnetic shell model were combined with thermal equations in calculating properties of both the sample and the reactor as a whole. Those proper-tics included the Q of the cavity, and power absorption distributions and temperature profiles in the sample under both steady state and transient conditions.

In later work [5], we treated a cylindrical sample in a cylindrical cavity using a cylindrical shell model. Exact formulas for normal mode frequencies, quality factors, electromagnetic fields and for power absorption distributions in the sample were derived under idealized conditions in which the cavity walls were assumed to be perfect electrical conductors.

This paper addresses the problem of extending the cylindrical shell model to calculate temperature profiles inside microwave reactors. This new theory contains several noteworthy features. First, the finite electrical conductivity of the cavity walls is taken into account accurately. Second, realistic values of thermal emissivity are taken into account at solid boundaries inside the cavity and at the cavity walls. Third, effects of both direct microwave heating of the sample and radiant heating of the sample by a microwave heated tube that surrounds it are included in the model. That is, hybrid heating of the sample can be accommodated in the model.

As in our earlier work a combination of analytic and numerical approached is used in solving the problem. The main elements of the theory will be described next. Then calculated results will be presented and discussed in the context of materials processing. Our conclusions will be presented in the final section.

TH EORY

The geometry of the cylindrical shell model is shown in Fig. 1 for the case where a microwave-heated tube surrounds the cylindrical sample. Interior regions of both the. sample and tube are partitioned into radially thin zones, but vacuum spaces are not subdivided. In each zone the complex dielectric constant is assumed to be uniform, but it may vary from one zone to another. 'l'he N+ 1^{th} zone is the curved cavity wall, which is infinitely thick in the model.

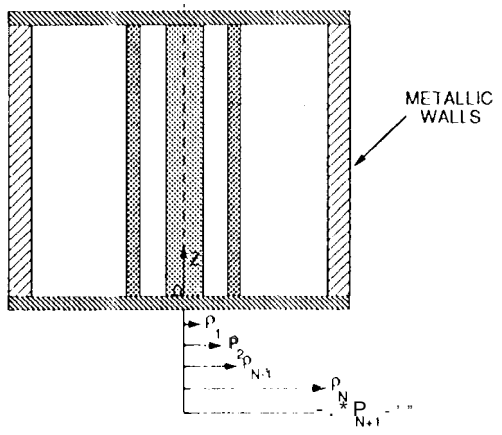

Fig. 1. Geometry of cylindrical shell model.

Solution of the electromagnetic problem was divided into two steps. In the first step, the flat end plates of the cavity were treated as perfect electrical conductors. Then by applying a technique described in our earlier work, we found, exact solutions of Maxwell's equations with harmonically varying fields $e^{-i\omega t}$ and subject to appropriate bounding conditions. The method of solution involved expanding the fields in each zone in terms of cylindrical Bessel functions J_ℓ and cylindrical Neumann functions Y_ℓ. In the curved cavity walls, zone N+1, the solutions can contain only outgoing waves

corresponding to cylindrical Hankel functions of the first kind, $H_\ell^{(1)} = J_\ell + iY_\ell$, since no energy propagates inward form infinity. Using this observation, we were able to include the curved cavity walls in the part of the model that could be treated exactly.

Normal mode frequencies, which were in general complex-valued, were calculated by finding the zeros of a complex-valued determinant of a certain 4x4 matrix, having 4 rows and 4 columns. Subsequently, the eigenfunctions of the 4x4 matrix were calculated, and these eigenfunctions provided input for applying a stepwise procedure to evaluate the expansion coefficients that occur in formulas for electromagnetic fields in each zone. For a TM_{0n0} mode the electric and magnetic fields in zone j are given by:

$$\boldsymbol{E}_n^j(\boldsymbol{r}) = 2\left[c_n^j J_0\left(\lambda_n^j \rho\right) + d_n^j Y_0\left(\lambda_n^j \rho\right)\right] z \tag{1}$$

$$\boldsymbol{H}_n^j(\boldsymbol{r}) = \frac{2ik_n^j}{\omega\mu_0}\left[c_n^j J_0'\left(\lambda_n^j \rho\right) + d_n^j Y_0'\left(\lambda_n^j \rho\right)\right]\theta . \tag{2}$$

Here c_n^j and d_n^j are expansion coefficients, and J_0' and Y_0' arc derivatives of functions with respect to their arguments. Also, (ρ, θ, z) are cylindrical coordinates with origin at the center of the bottom end plate of the cavity. These formulas for the fields can be used to find formulas that can be used to evaluate the power absorbed in each zone and the time average energy stored in each zone.

In the second step of the electromagnetic problem, the finite conductivity of the cavity end plates was taken into account using the surface resistance approximation. In this approximation, the time average microwave power W absorbed at a surface So is given by

$$W = \frac{1}{2} R_S \int_{S_0} \boldsymbol{H}_t(\boldsymbol{r}) \bullet \boldsymbol{H}_t^*(\boldsymbol{r}) ds . \tag{3}$$

$\boldsymbol{H}_t(\boldsymbol{r})$ is the tangential component of the magnetic field found in Step 1, and R_S is the surface resistance given by

$$R_S = \frac{1}{\sigma\delta_S}, \tag{4}$$

where σ is the electrical conductivity of the end plate material and δ_S is the penetration depth

$$\delta_s = \left[\frac{2}{\omega' \mu_0 \sigma}\right]^{\frac{1}{2}}. \qquad (5)$$

The integral in Eq. (3) can be evaluated analytically for the case we are considering, and this provided an explicit formula for power adsorption in the two end plates.

The formulas described so far can be used to accurately calculate total time average power absorbed inside the cavity and in the cavity walls. The formulas can also be used to calculate the total Q of the cavity containing the sample and the contributions to the total Q and total absorbed power made by the sample, by a tube that may surround the sample, and by the cavity walls.

Next the solution of the electromagnetic problem was combined with a thermal model to calculate temperature profiles. Under steady state conditions, the general forms of the thermal equations are

$$\nabla \cdot q(r) = P(r) \qquad (6)$$

$$q(r) = -\kappa \nabla T(r). \qquad (7)$$

In each zone the heat source P(r) was taken to be a constant equal to the microwave power absorbed per unit volume averaged over the volume of the zone and averaged over time. The thermal conductivity κ was approximated as a linear function of temperature in each zone. The continuity of K at every zone boundary interior to the sample or tube was enforced. In the model, heat is transferred across the surfaces of the sample, tube, and cavity walls by thermal radiation only, and that is calculated in a gray body approximation.

The interior faces of the end plates are assumed to be perfect reflectors of thermal radiation, a condition that can be closely approximated in a real reactor by using highly polished, shiny surfaces. This assumption greatly simplifies the problem of solving the thermal equations. More specifically, it implies that the thermal radiation formula for two infinitely long cylinders, viz.,

$$Q = \frac{\sigma_{sB} A_1 \left(T_1^4 - T_2^4\right)}{\frac{1}{\varepsilon_1} + \frac{\rho_1}{\rho_2}\left(\frac{1}{\varepsilon_2} - 1\right)}, \qquad (8)$$

can be applied here.

The steady state thermal equations have been solved analytically for each zone, and these solutions must be used with appropriate boundary conditions on temperature

and heat current at zone interfaces. The formal solution of the thermal problem must be combined self-consistently with the electromagnetic equations. This can be accomplished by using an iteration procedure. The thermal and electromagnetic equations are coupled in two ways: (i) the complex dielectric constant is in general a function of temperature; and (ii) power absorbed in each zone is a source of heat in the thermal equations. Some results calculated with this self-consistent procedure will be discussed next.

DISCUSSION

A parametric study of the temperature within a cylindrical cavity containing a cylindrical rod aligned along the cavity axis and a tube concentric to the sample was performed using this new theory. "I'he cavity radius, ρc = 4.69 cm, and length, L= *6.63 cm,* correspond to a 2.45 GHz resonant frequency for an empt y cavity TM_{010} mode. These dimensions are the same as in our previous microwave power absorption study [5]. In this investigation, the temperature dependent properties of alumina were used for all rods and tubes [6,7]. The calculations were performed on a Cray computer generally using *8* zones for the rod and 2 to 8 zones for the tube. The parameters computed included the electric field strength at the surface of the rod, the temperature profile within the rod and tube, the power absorbed in the cavity walls, rod and tube, and the resonant frequency of the cavity.

A nominal set of experimental parameters was chosen for the present calculations. The nominal alumina rod radius and emissivity values were a =- 0.2 cm ($a/\rho c$ = ().043) and $\varepsilon_s = 0.31$ respectively. The input power was P = 100 W into the cavity for the TM_{010} mode and the cavity walls were copper with an emissivity of&w = ().()25. The tube thickness, mid-radius and inner and outer surface emissivities were d = O. 1 cm, r_{mid} = ***0.4*** cm and $\varepsilon_{t_i} = \varepsilon_{t_o}$ = 0.31 respectively. The following graphs correspond to varying one of the parameters while holding the remaining nominal parameters constant unless stated otherwise.

The temperature profile within the rod using the nominal parameter set is shown in Fig. 2 for the first three TM_{0n0} modes. For this small diameter rod, the average temperature and the temperature gradient within the rod both increase with mode number. The average rod temperature for the TM_{030} was calculated to be ≈ 150 C higher than the TM_{010} while the temperature gradient was 35 C for the TM_{030} mode compared to only 20 C for the TM_{010} mode. These gradients become significantly larger as the rod diameter was increased.

The cavity wall emissivity plays a very important role in determining the final temperature of the rod as shown in Fig. 3. As the wall emissivity approaches zero, more of the energy, radiated to the. wall from the tube and the rod, is reflected back leading to an increase in the rod (and tube) steady state temperature. The presence of the tube significantly increases the rod temperature for larger wall emissivities (> 0.05).

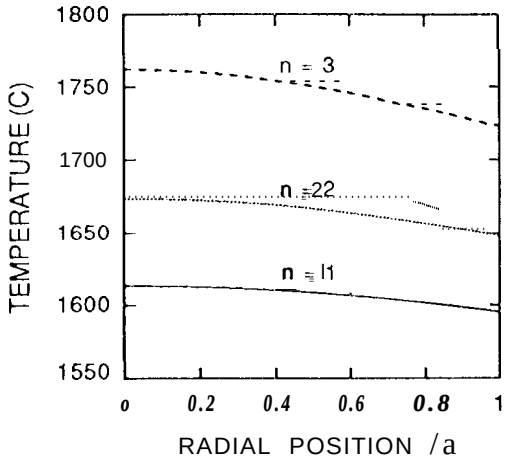

Fig. 2. Rod temperature profile for three lowest TM0n0 modes.

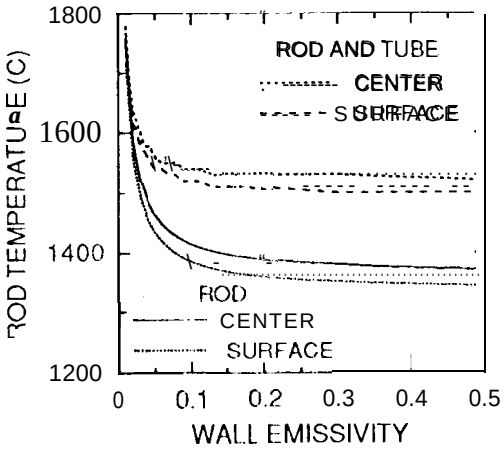

Fig. 3. Rod center and surface temperatures versus wall emissivity with and without the tube.

The rod emissivity effects the rod temperature in a manner similar to the cavity wall emissivity. Figure **4** shows the dependence of the rod center and surface temperatures on the rod emissivity with and without the tube present. Again the rod

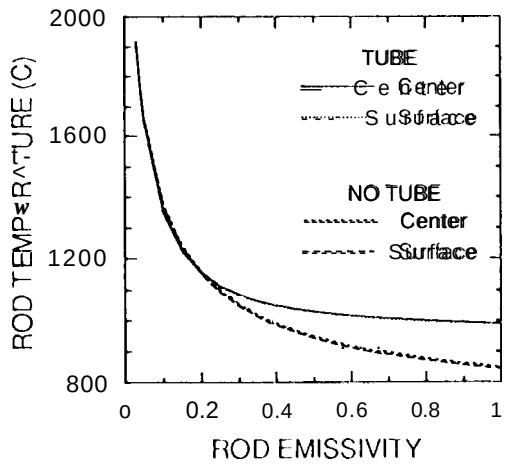

Fig. 4. Rod center and surface temperatures versus rod emissivity with and without the tube.

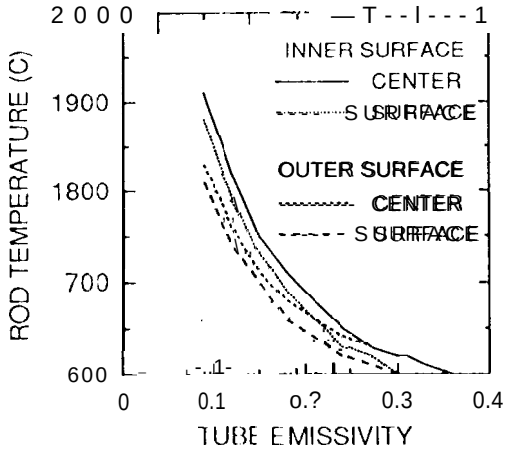

Fig. 5. Rod center and surface temperatures versus inner and outer surface tube emissivity.

temperature rises sharply as the emissivity is reduced. However, in contrast to the cavity wall emissivity, the tube increases the rod temperature only at higher emissivity values (> 0.25).

The effect of the emissivity of the inner and outer surfaces of the tube on the rod temperature was also investigated. Figure 5 shows the strong dependence of the rod center and surface temperatures on the tube emissivities. The tube inner surface emissivity has a slightly stronger effect on the rod temperatures than the tube outer surface. These calculations indicate that the rod temperature can be increased by almost 300 C by reducing the emissivity of the alumina tube inner surface to O. 1. This reduction could possibly be accomplished by coating the tube with a low emissivity material that adheres to alumina at high temperatures.

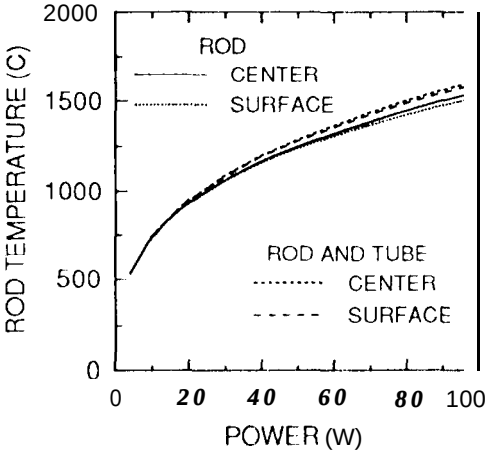

Fig. 6. Rod center and surface temperatures versus power with and without tube.

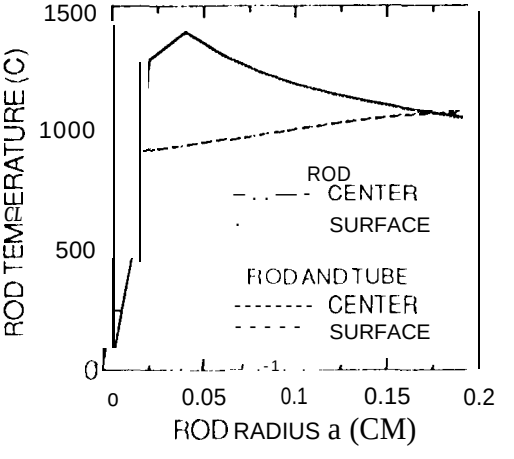

Fig. '/. Rod center and surface temperatures versus rod radius with and without tube.

Figure 6 shows the center and surface temperatures of the rod with and without the tube present as a function of the power introduced into the microwave cavity. With the tube present, there is only a small 50 C increase in the center and surface temperatures at a 100 W power level. 'l'he fact that the tube has little effect on the rod temperature is associated with the chosen nominal parameter set. The effect of the tube becomes more significant as the rod radius is reduced as shown in Fig. 7 where the power has been fixed at 30 W. 'l'he presence of the tube actually reduces the temperature of the rod for radii in the range ().()17 cm < a < 0.17 cm. For smaller or larger rods, the tube increases the temperature of the rod. '1'here is a critical rod radius (a ≈ 0.025 cm) that leads to a maximum isolated rod temperature (≈ 1480 C). Of particular interest is the small rod region, below the critical radius, which is relevant (o the microwave. processing of fibers. In this region the temperature of an isolated fiber is significantly reduced from the peak temperature.

However. the fiber temperature remains relatively constant (900 C < T < 1100 C) with a tube surrounding' [he fiber.

From the results of the nominal parameter set study, we have chosen an optimum parameter set for heating a rod. This parameter set only differed from the nominal set in that the TM_{030} mode is used and the emissivity of the tube surfaces is set at 0.1 which is a technically achievable value. Figure *8* shows the rod center and surface temperatures as a function of power into the cavity for the nominal 0.2 cm radius rod and a 20 pm radius fiber that is 100 times smaller. This calculation indicates that with this optimum parameter set the rod can be heated to melting with less than 80 watts. Furthermore, the fiber can reach a temperature above 1500 C using this same power level.

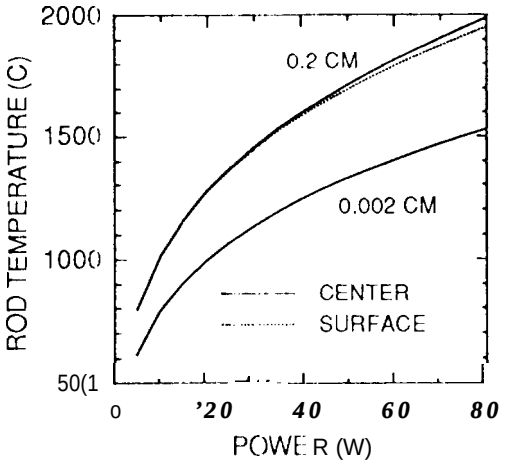

Fig. 8. Rod and fiber center and surface temperatures versus power for an optimum parameter set

CONCI,IJS1ONS

We have developed a steady state microwave model for a cylindrical rod situated along the entire axis of a cylindrical cavity. The model was applied to the microwave heating of an isolated rod as well as the hybrid heating of a rod surrounded by a microwave heated tube. A parametric microwave heating study was performed for samples ranging from fibers to large rods. This study demonstrated that by optimizing the experimental parameters, efficient microwave/hybrid heating of fibers and rods can be achieved. These results should support future economical development of commercial microwave processing applications.

ACKNOWLEDGMENT

The research described in this article was carried out at the Jet Propulsion Laboratory, California Institute of '1'ethnology, under contract with **the** National Aeronautics and Space Administration.

REFERENCES

1. I 1. W. Jackson and M. Barmatz, "Microwave Absorption by a 1 ossy Dielectric Sphere in a Rectangular Cavity," J. Appl. Phys. 70, 5193 (1991).

2. H.W. Jackson and M. Barmatz, "Method for Calculating and Observing Microwave Absorption by a Sphere in a Single Mode Rectangular Cavity," Ceramic Transactions 21, 261, (1991).

3. M. Barmatz and H. W. Jackson, "Steady State Temperature Profile in a Sphere Heated by Microwaves," MRS Symp. Proc., Vol. 269, pp. 97-103 (1992).

4. H. W. Jackson, M. Barmatz and P. Wagner, "Transient Temperature Behavior of a Sphere Heated by Microwaves," Ceramic Transactions, 36, 189, (1993).

5. H.W. Jackson, M. Barmatz, and P. Wagner, "Microwave Power Absorption Profile in a Cylindrical Sample Contained in a Resonant Cylindrical Cavity," MRS Symp. Proc., Vol. 347, pp. 317-323 (1994).

6. H. Fukushima, T. Yamanaka and M. Matsui, J. of Japan Soc. of Prec. Eng. 53, 743 (1987).

7. Y. S. Touloukian, Thermophysical Properties of Matter, (IFI/Plenum, New York - Washington, 1972), Vol. 8,. p. 98.